Thermally enhanced photoluminescence and temperature sensing properties of $Sc_2W_3O_{12}$:Eu^{3+} phosphors

Yu-De Niu(牛毓德), Yu-Zhen Wang(汪玉珍), Kai-Ming Zhu(朱凯明), Wang-Gui Ye(叶王贵), Zhe Feng(冯喆), Hui Liu(柳挥), Xin Yi(易鑫), Yi-Huan Wang(王怡欢), and Xuan-Yi Yuan(袁轩一)†

Beijing Key Laboratory of Optoelectronic Functional Materials & Micro-nano Devices, Department of Physics, Renmin University of China, Beijing 100872, *China*

(Received 22 March 2022; revised manuscript received 15 May 2022; accepted manuscript online 18 May 2022)

Recently, lanthanide-ion-doped luminescent materials have been extensively used as optical thermometry probes due to their fast responses, non-contact, and high sensitivity properties. Based on different responses of two emissions to temperature, the fluorescence intensity ratio (FIR) technique can be used to estimate the sensitivities for assessing the optical thermometry performances. In this study, we introduce different doping concentrations of Eu^{3+} ions into negative thermal expansion material $Sc_2W_3O_{12}$ to increase the thermal-enhanced luminescence from 373 K to 548 K, and investigate the temperature sensing properties in detail. All samples can exhibit their good luminescence behaviors thermally enhanced. The emission intensity of $Sc_2W_3O_{12}$:6-mol% Eu^{3+} phosphor reaches 147.8% of initial intensity at 473 K. As the Eu^{3+} doping concentration increases, the resistance of the sample to thermal quenching decreases. The FIR technique based on each of the transitions $^5D\rightarrow {}^7F_1$ (592 nm) and $^5D\rightarrow {}^7F_2$ (613 nm) of Eu^{3+} ions demonstrates a maximum relative temperature sensitivity of 3.063% K^{-1} at 298 K for $Sc_2W_3O_{12}$:6-mol% Eu^{3+} phosphor. The sensitivity of sample decreases with the increase of Eu^{3+} concentration. Benefiting from the thermal-enhanced luminescence performance and good temperature sensing properties, the $Sc_2W_3O_{12}$:Eu^{3+} phosphors can be used as optical thermometers.

Keywords: photoluminescence, $Sc_2W_3O_{12}$:Eu^{3+}, negative lattice expansion, thermal-enhanced luminescence

PACS: 87.15.mq, 32.50.+d, 78.55.–m **DOI:** 10.1088/1674-1056/ac70b8

1. Introduction

Lanthanide ions-doped luminescence phosphors have been widely used in displays,[1] lighting,[2] and sensors.[3] Therein optical thermometry based on luminescence materials has attracted considerable attention due to the fast response, non-contact, and high sensitivity.[4,5] By employing the fluorescence intensity ratio (FIR) of thermally coupled energy levels (TCELs) or non-thermally coupled energy levels (NTCELs), the temperature sensing properties could be obtained.[6–8] The potential of luminescence materials to be applied to optical thermometers was evaluated by absolute sensitivity (S_a) and relative sensitivity (S_r).[7,9] For Eu^{3+}-doped materials, several pairs of emissions have been executed for FIR technique due to the abundant energy levels of Eu^{3+} ions.[10,11] Liang *et al.* revealed that $^5D_1/^5D\rightarrow {}^7F_1$ TCELs (541 nm/590 nm) and $(^5D\rightarrow {}^7F_2)/(^5D_1 \rightarrow {}^7F_1)$ NTCELs (625 nm/541 nm) of Eu^{3+} ions in $LiNbO_3$ single crystals can be devoted to the optical temperature sensor based on the FIR method, and the maximum values of S_a are 7×10^{-4} K^{-1} and 24×10^{-4} K^{-1}, respectively.[12] In addition, Nikolić *et al.* developed $(^5D_1 \rightarrow {}^7F_1)/(^5D\rightarrow {}^7F_2)$ NTCELs (533 nm/611 nm) in Gd_2O_3:Eu phosphors for thermography, and the maximum value of S_a was 7×10^{-4} K^{-1} at 800 K.[13]

However, the current phosphors used for optical temperature measurement inevitably face the problem caused by thermal quenching. With the increase of temperature, the luminescence intensity of phosphors would be significantly reduced.[14] This will seriously hinder the application of optical thermometry in high-temperature environment. So far, many efforts have been devoted to resisting the thermal quenching.[15–17] Negative thermal expansion (NTE) luminescence materials have triggered off much concern due to the resistance of volume expansion with temperature increasing, which is a distinct advantage for practical applications.[18] In particular, the energy collection by activators could be promoted by the reversible lattice shrinkage and deformation, resulting in the thermal-enhanced emissions.[18,19] For instance, Zou *et al.* reported that the luminescence of NTE upconversion $Yb_2W_3O_{12}$:Er crystal increases more than 12 times when temperature reaches to 573 K.[19] Besides, Zhou *et al.* demonstrated that the NTE effect of $Zr(WO_4)_2$:Eu phosphors can effectively inhibit the emission loss of thermal quenching. Comparing with the scenario at room temperature, the luminescence intensity can be enhanced by 130% at 373 K.[20] Furthermore, the investigation on luminescence properties of lanthanide ions-doped NTE $Sc_2W_3O_{12}$ material was carried out. Li *et al.* reported Eu^{3+}-doped $Sc_2W_3O_{12}$ phosphors with good thermal-quenching resistance at low temperature (97 K–280 K).[21] Recently, Wang *et al.* demonstrated that the emission intensities of $Sc_2W_3O_{12}$:Eu^{3+} ($x = 0.01$–0.10) are abnormally enhanced with temperature increasing up to 473 K.[22] However, the application of $Sc_2W_3O_{12}$:Eu^{3+} phosphor in the field of optical temperature measurement is seldom reported.

†Corresponding author. E-mail: yuanxuanyi@ruc.edu.cn

© 2023 Chinese Physical Society and IOP Publishing Ltd

In this work, we successfully synthesize $Sc_2W_3O_{12}$ phosphors with high Eu^{3+} concentration in a range of 6 mol%–34 mol%. The luminescent thermal properties of $Sc_2W_3O_{12}$:Eu^{3+} with various concentrations and their applications in the field of optical temperature measurement are systematically investigated. Under the excitation at 264 nm, the bright red emission of $Sc_2W_3O_{12}$:Eu^{3+} phosphors exhibit their good luminescences thermally enhanced from 373 K to 548 K. Specifically, the $Sc_2W_3O_{12}$:6-mol% Eu^{3+} phosphors present 147.8% of initial intensity at 473 K. Besides, owing to the different responses of emissions at 592 nm ($^5D\rightarrow {}^7F_1$) and 613 nm ($^5D\rightarrow {}^7F_2$) to temperature, $Sc_2W_3O_{12}$:Eu^{3+} phosphors show excellent temperature sensing properties based on the FIR technique. The estimated maximum S_a and S_r are 6.872×10^{-3} K^{-1} and 3.063% K^{-1} at 298 K, respectively. In addition, this thermally enhanced luminescence performance of phosphors reduces the difficulty in implementing the luminescence detection at high temperature. These results verify the availability of lanthanide ions-doped NTE luminescence materials against thermal quenching, and demonstrate their applications in optical thermometers.

2. Experiment

2.1. Sample preparation

The $Sc_2W_3O_{12}$ phosphors were prepared by high-temperature solid-state reaction. The Sc_2O_3 (scandium oxide, 99.99%, Aladdin), WO_3 (tungsten trioxide, 99.99%, Aladdin) and Eu_2O_3 (europium oxide, 99.99%, Aladdin) were used as raw materials. After being weighed according to stoichiometry ratio, the raw materials were stirred in planetary ball mill for 12 h. After the obtained slurry is dryed, the mixture was pressed into thin discs each with a diameter of 15 mm and a thickness of 2 mm, and they were sintered in a box furnace at 1100 °C for 4 h. The sintered samples can be used for subsequent tests after being carefully ground in an agate mortar.

2.2. Characterization

The x-ray diffraction (XRD) of all samples were identified by the D8 ADVANCE x-ray diffractometer of the Bruker corporation with Cu-$K\alpha$ radiation ($\lambda = 1.5406$ Å). Morphologies were characterized on a field-emission scanning electron microscope (FE-SEM, JSM-6700 F). Photoluminescence (PL) and PL excitation (PLE) spectra were measured by using a fluorescence spectrophotometer (F-7000, Hitachi) equipped with a high-temperature fluorescence controller (TAP-02).

3. Results and discussion

3.1. Phase and morphology analysis

Figure 1(a) shows the XRD results of $Sc_2W_3O_{12}$:x-mol% Eu^{3+} phosphors (x = 6, 10, 14, 18, 22, 26, 30, 34). The diffraction peaks of samples are well matched with the standard patterns of $Sc_2W_3O_{12}$ (PDF#89-4690), demonstrating the successful synthesis of $Sc_2W_3O_{12}$ pure phase.[23]

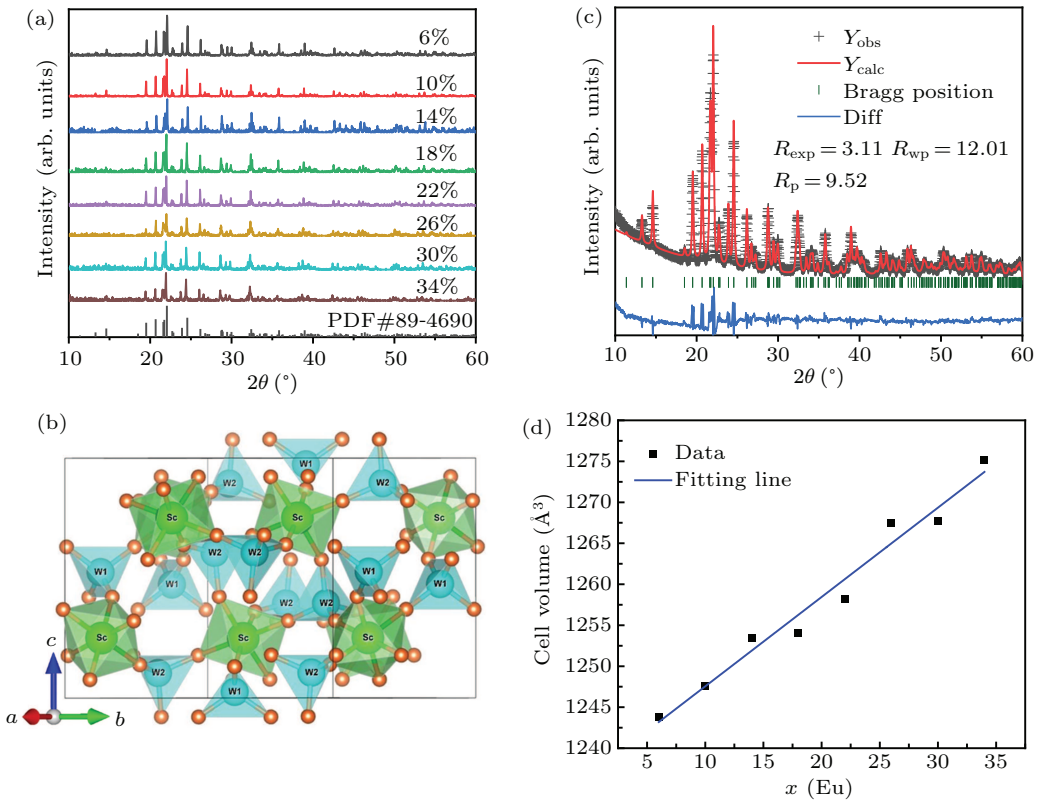


Fig. 1. (a) XRD patterns of $Sc_2W_3O_{12}$:x-mol% Eu^{3+} (x = 6, 10, 14, 18, 22, 26, 30, 34) at room temperature (RT). (b) Schematic diagram of crystal structure of orthorhombic $Sc_2W_3O_{12}$ and Eu^{3+} ions substitution diagram. (c) Results of Rietveld refinement of XRD pattern of $Sc_2W_3O_{12}$:6-mol% Eu^{3+} phosphors. (d) Cell volume of $Sc_2W_3O_{12}$ with various Eu^{3+} doping concentrations.

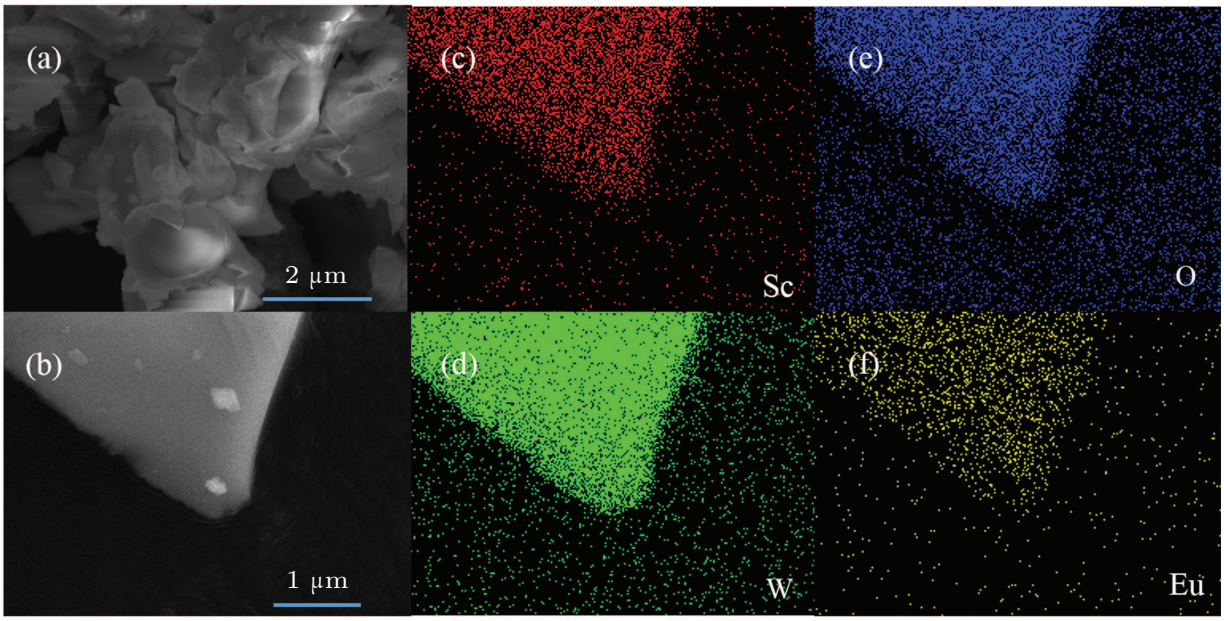


Fig. 2. (a) and (b) SEM images of $Sc_2W_3O_{12}$:22-mol% Eu^{3+} phosphors. (c)–(f) Element mapping images of Sc, W, O, and Eu snatched from the region indicated in panel (b), respectively.

Figure 1(b) displays the crystal structure of $Sc_2W_3O_{12}$, consisting of tetrahedral WO_4 and octahedral ScO_6 units connected by oxygen. The Rietveld refinement results indicate the orthorhombic structure with space group of *Pnca* (No. 60) of $Sc_2W_3O_{12}$:Eu^{3+} phosphors at room temperature as shown in Fig. 1(c) and Fig. S1. The corresponding fitting baseline of Fig. 1(c) is given in Fig. S2. According to the refinement, we calculate the lattice parameters and corresponding volumes of various Eu^{3+}-doped $Sc_2W_3O_{12}$ phosphors and the results are presented in Fig. 1(d) and Fig. S3, respectively. Obviously, the volume of the crystal gradually increases with the augment of doping concentration of Eu^{3+} ions. This can be attributed to the fact that Eu^{3+} (0.95 Å) with larger radius occupies the position of Sc^{3+} (0.885 Å).[24]

The morphologies are recorded by SEM images in Fig. 2(a). The average size of $Sc_2W_3O_{12}$:Eu^{3+} particles ranges from 1 μm to 5 μm. Figures 2(c)–2(f) show the element mappings of Sc, W, O, and Eu^{3+} in $Sc_2W_3O_{12}$:22-mol% Eu^{3+} phosphors snatched from the region indicated in Fig. 2(b), respectively. It can be observed that the elements are uniformly distributed in $Sc_2W_3O_{12}$: Eu^{3+} phosphors.

3.2. PL properties at room temperature

In order to study the luminescence properties of $Sc_2W_3O_{12}$:Eu^{3+} phosphors, we measure the PLE spectra of samples with different doping concentrations of Eu^{3+} ions at room temperature. The measurements are monitored at 613-nm emission, and the results are presented in Fig. 3(a). In general, the excitation spectra of samples can be mainly divided into two parts. The broadband in the ultraviolet region (200 nm–350 nm) derives from the charge transfer band (CTB) of tungstate ions.[20,21,25] And the other sharp weak peaks at 318 nm, 360 nm, 384 nm, 393 nm, and 464 nm originate from the transitions $^7F\rightarrow{}^5D_4$, $^7F\rightarrow{}^5L_7$, $^7F\rightarrow{}^5L_6$, $^7F\rightarrow{}^5D_3$, and $^7F\rightarrow{}^5D_2$ of Eu^{3+} ions, respectively. Figure 3(b) illustrates the emission peaks of samples with different Eu^{3+} concentrations under 264-nm excitation. And the peaks located at 592 nm, 613 nm, and 653 nm result from the $^5D\rightarrow{}^7F_1$, $^5D\rightarrow{}^7F_2$, and $^5D\rightarrow{}^7F_3$ transition of Eu^{3+} ions respectively. With the increase of Eu^{3+} concentration, the emission intensities initially increase and reach their corresponding maximum values when $x = 22$, and then decrease due to the concentration quenching effect. The emission intensities of 592 nm and 613 nm are normalized to the emission of $Sc_2W_3O_{12}$:22-mol% Eu^{3+} phosphors, and their variations with Eu^{3+} concentration is depicted in Fig. 3(c). It can be observed that the emission intensity of 592 nm varying with Eu^{3+} concentration is basically consistent with that of 613 nm. To explore the interaction type of the activator in $Sc_2W_3O_{12}$:Eu^{3+} phosphors, the Dexter theory is employed in Fig. 3(d):[26–30]

$$\ln\left(\frac{I}{x}\right) = A - \frac{\theta}{3}\ln(X), \tag{1}$$

where I is the integral fluorescence intensity, x represents the doping concentration of Eu^{3+}, A is a constant, and θ refers to the eigenvalue related to the interaction type ($\theta = 3$, 6, 8, 10 corresponding to exchange, dipole–dipole, dipole–quadrupole, quadrupole–quadrupole interactions, respectively).[28] According to the fitting result, the θ value is about 3.0199, suggesting that the concentration quenching of activators in $Sc_2W_3O_{12}$:Eu^{3+} phosphors is derived from exchange interaction.

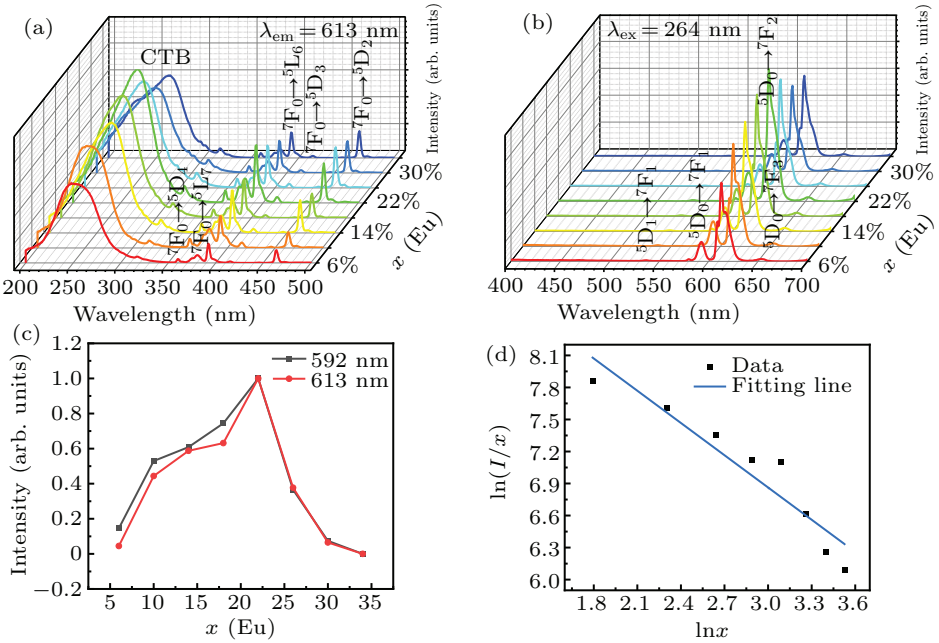


Fig. 3. (a) PLE (emitted at 613 nm) and (b) PL (excited by 264 nm) spectra of $Sc_2W_3O_{12}$:*x*-mol% Eu^{3+} ($x = 6$, 10, 14, 18, 22, 26, 30, 34) phosphors at room temperature. (c) Curves of normalized luminescence intensity at 592 nm and 613 nm varying with doping concentrations. (d) Plot of $\ln(I/x)$ *versus* $\ln x$, and the slope of the fitting line is 1.0065.

3.3. Temperature-dependent PL performances

Taking the $Sc_2W_3O_{12}$:6-mol% Eu^{3+} sample for example, the negative thermal expansion behavior of the $Sc_2W_3O_{12}$ matrix is demonstrated. The Rietveld refinement results (Fig. S4) of variable temperature XRD patterns presented in Fig. 4(a) verify the NTE of sample, and the refined lattice parameters as well as the cell volume values are illustrated in Figs. 4(b) and 4(c), respectively. Notably, the *in-situ* XRD patterns demonstrate the stable orthorhombic phase of $Sc_2W_3O_{12}$ at various temperatures. And the lattice of the sample shrinks in the direction of the *a* axis and *c* axis, and expands slightly in the direction of *b* axis from room temperature to 573 K. Consequently, the cell volume expands until 373 K and further contracts with temperature rising, which indicates the NTE of $Sc_2W_3O_{12}$:6-mol% Eu^{3+} phosphors ranging from 373 K to 573 K. As is well known, changes in the crystal structure of materials will inevitably affect its luminescent properties. The temperature-dependent emission spectra of $Sc_2W_3O_{12}$:6-mol% Eu^{3+} phosphors under the excitation at 264 nm are delineated in Fig. 4(d). Figure 4(e) shows that the emission intensity at 613 nm maintains 86.61% of initial intensity at 373 K, then abnormally rapidly increases with temperatures reaching up to 548 K and the highest emission intensity arrives at 147.8% of initial intensity at 473 K. Moreover, the emission at 592 nm presents a similar trend to that at 613 nm. It is noteworthy that the luminescence intensity attenuating with temperature rising from RT to 373 K can be ascribed to the thermal quenching, and the enhanced luminescence is due to the NTE effect that occurs in a temperature range from 373 K to 548 K. In general, the bridging oxygen of Sc–O–W undergoes the transverse vibrations, leading to the coupled tilting of framework polyhedra.[23] As a result, the crystal structure of $Sc_2W_3O_{12}$:Eu^{3+} phosphors grows denser and the energy collection of activator is promoted, demonstrating the stronger thermal-quenching resistance of luminescence.[19,22] In addition, we measure the PL spectra of $Sc_2W_3O_{12}$:*x*-mol% Eu^{3+} ($x = 10$, 14, 18, 22, 26, 30) phosphors (Fig. S5). As shown in Fig. 4(f), it is obvious that the thermal-quenching resistance of $Sc_2W_3O_{12}$:Eu^{3+} decreases with the increase of Eu^{3+} concentration at 298 K–548 K. At low Eu^{3+} concentrations (6 mol%–10 mol%), the PL intensity of the sample can maintain about 85% of initial intensity (in the green dashed box of Fig. 4(f)). However, at medium Eu^{3+} concentrations (14 mol%–18 mol%, in the orange dashed box) and high doping concentrations (26 mol%–30 mol%, in the blue dashed box), the PL intensities of the sample can be reduced to about 80% and 67% of initial intensity, respectively. On the other hand, the onset temperature at which luminescence enhancement begins to appear also tends to increase with the Eu^{3+} doping concentration increasing.

To investigate the temperature sensing properties of $Sc_2W_3O_{12}$:*x*-mol% Eu^{3+} phosphors, the contributions of TCEL's emissions at 592 nm and 613 nm are measured by the FIR technique. The FIR value *R* is defined as $R = I_{592\ \mathrm{nm}}/I_{613\ \mathrm{nm}}$, and depicted in Fig. 5(a) and Fig. S6. The relationship between *R* value and temperature can be given by the following function:[31]

$$R = A\exp(-B/T) + C. \tag{2}$$

Here, *A*, *B*, and *C* are the parameters related to the sample. After being fitted by a mono-exponential function, the absolute

sensitivity and relative sensitivity are calculated. Generally, these two indicators are employed to evaluate the temperature sensing properties of luminescence materials. They can be estimated by the following equations:[32–34]

$$S_{\mathrm{a}} = \frac{\mathrm{d}R(T)}{\mathrm{d}T}, \tag{3}$$

$$S_{\mathrm{r}} = \frac{1}{R}\frac{\mathrm{d}R(T)}{\mathrm{d}T}. \tag{4}$$

The calculated sensitivities are shown in Fig. 5(b) and Fig. S6. The corresponding mathematical expressions are listed in Table S1. Comparing the maximum values of S_{a} and S_{r} of samples under different Eu^{3+} concentrations in Fig. 5(c), we can see that the sensitivity of the sample decreases with the increase of Eu^{3+} concentration. When the concentration reaches 22%, the maximum sensitivity begins to increase again. Of all samples in this work, the sensitivity of the sample with 6-mol% Eu^{3+} is the highest, and its maximum values of S_{a} and S_{r} can reach 6.872×10^{-3} K^{-1} and 3.063% K^{-1} at 298 K, respectively. In addition, the values of S_{a} and S_{r} maintain the downward trends with temperature increasing, which implies possible preferable temperature sensing properties in low-temperature region.

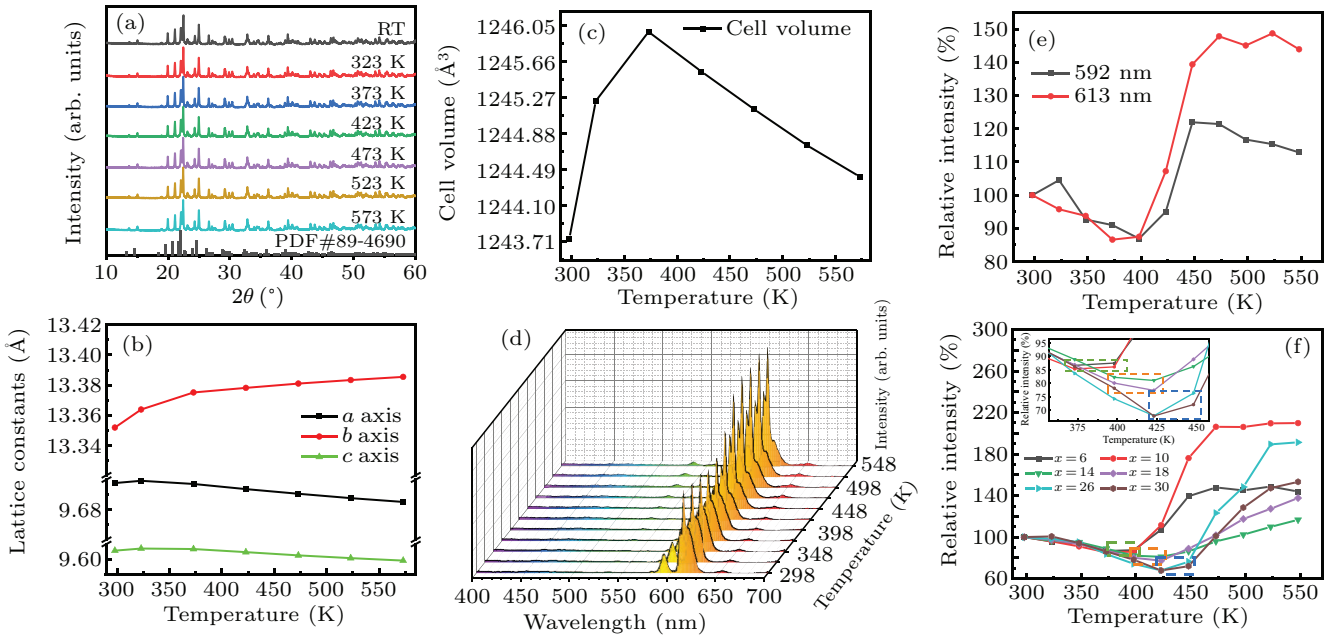


Fig. 4. (a) Temperature-dependent XRD patterns of $Sc_2W_3O_{12}$:6-mol% Eu^{3+} phosphors. (b) Lattice constants and (c) cell volume values of sample changing with temperatures. (d) Temperature-dependent PL spectra of $Sc_2W_3O_{12}$:6-mol% Eu^{3+} under 264-nm excitation. (e) Relative intensity at 592-nm and 613-nm emissions of $Sc_2W_3O_{12}$:6 at.% Eu^{3+} varying with temperatures. (f) Relative intensity at 613 nm of $Sc_2W_3O_{12}$:x-mol% Eu^{3+} ($x = 6$, 10, 14, 18, 22, 26, 30) varying with temperatures, with inset showing enlarged part of curves at temperatures in a range of 350 K–475 K.

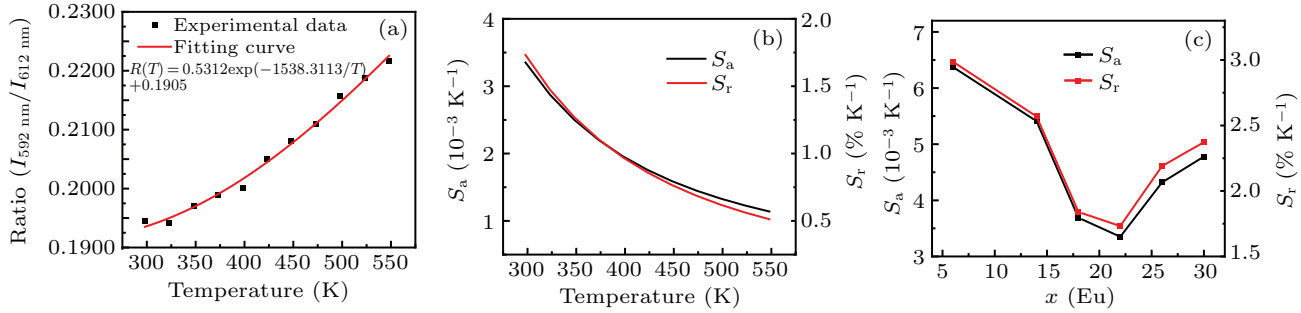


Fig. 5. The temperature-dependent (a) PL intensity ratio of 593 nm and 613 nm with fitting results and (b) absolute sensitivity (S_{a}) and relative sensitivity (S_{r}) values of $Sc_2W_3O_{12}$:22-mol% Eu^{3+} phosphors, and (c) maximum values of S_{a} and S_{r} varying with doping concentrations.

4. Conclusions

In this work, we synthesized negative thermal expansion $Sc_2W_3O_{12}$:Eu^{3+} phosphors by the conventional solid-state method. The XRD results reveal that the pure orthorhombic phase can be maintained when being doped with various concentrations of Eu^{3+} ions or elevating temperature. Furthermore, the SEM images and elemental mappings confirm the uniform distributions of Sc, W, O, and Eu ions in samples. Under the 264-nm irradiation, the bright red emission can be observed and the quenching concentration of Eu^{3+} ions is 22 mol% due to the exchange interaction. When the temperature increasing from 298 K, the bridging oxygen of Sc–O–W undergo transverse vibrations, leading to the coupled tilting of framework polyhedron. And the lattices of $Sc_2W_3O_{12}$:Eu^{3+}

phosphors expand until 373 K and then contract with temperature rising up to 548 K. The emission intensity is abnormally rapidly enhanced with increasing temperature, which is derived from the enhanced energy collection of activators by lattice shrinkage and deformation. The capability of anti-thermal quenching decreases with increasing Eu^{3+} doping concentration. In addition, resulting from the different responses of emissions at 592 nm ($^5D\rightarrow {}^7F_1$) and 613 nm ($^5D\rightarrow {}^7F_2$) to temperature, $Sc_2W_3O_{12}$: Eu^{3+} phosphors can be used as optical thermometers based on the FIR technique. The estimated maximum values of S_a and S_r of $Sc_2W_3O_{12}$:6-mol% Eu^{3+} phosphors are 6.872×10^{-3} K^{-1} and 3.063% K^{-1} at 298 K, respectively, These results demonstrate that the $Sc_2W_3O_{12}$:Eu^{3+} phosphors can be used as optical thermometers due to the good temperature sensing properties and thermal-enhanced luminescence performance.

Acknowledgement

Project supported by the National Natural Science Foundation of China (Grant No. 51872327).

References

[1] Zhao M, Liao H X, Ning L X, Zhang Q Y, Liu Q L and Xia Z G 2018 *Adv. Mater.* **30** 1802489
[2] Huang X, Zhang W T, Wang X M, Zhang J Y, Gao X and Du H Y 2022 *J. Colloid. Interf. Sci.* **608** 3204
[3] Tang W, Zuo C D, Li Y K, Ma C Y, Yuan X Y, Wen Z C and Cao Y G 2021 *J. Mater. Chem. C* **9** 15112
[4] Wang Y Z, Wang Y A, Ma C Y, Li Y B, Zhao C, Ye W G, Wen Z C, Yuan X Y and Cao Y G 2021 *J. Materi. Chem. C* **9** 16626
[5] Kolesnikov I E, Kalinichev A A, Kurochkin M A, Mamonova D V, Kolesnikov E Y, Kurochkin A V, Lähderanta E and Mikhailov M D 2017 *J. Lumin.* **192** 40
[6] Yuan N, Liu D Y, Yu X C, Sun H X, Ming C G, Wong W H, Song F, Yu D Y, Pun E Y B and Zhang D L 2018 *Mater. Lett.* **218** 337
[7] Suo H, Zhao X Q, Zhang Z Y, Wang Y, Sun J S, Jin M K and Guo C F 2020 *Laser Photon. Rev.* **15** 2000319
[8] Zheng H, Chen B J, Yu H Q, Zhang J S, Sun J S, Li X P, Sun M, Tian B N, Fu S B, Zhong H, Dong B, Hua R N and Xia H P 2014 *J. Colloid Interf. Sci.* **420** 27
[9] Wang C L, Jin Y H, Zhang R T, Yao Q and Hu Y H 2022 *J. Alloys Compd.* **894** 162494
[10] Ye W G, Zhao C, Shen X F, Ma C Y, Deng Z H, Li Y B, Wang Y Z, Zuo C D, Wen Z C, Li Y K, Yuan X Y, Wang C and Cao Y G 2021 *ACS Appl. Electron. Mater.* **3** 1403
[11] Wade S A, Collins S F and Baxter G W 2003 *J. Appl. Phys.* **94** 4743
[12] Liang Z, Qin F, Zheng Y D, Zhang Z G and Cao W W 2016 *Sensor. Actuat. A-Phys.* **238** 215
[13] Nikolić M G, Al-Juboori A Z, Dordević V and Dramićanin M D 2013 *Phys. Scripta* **T157** 014056
[14] Cheng Y, Wang Y B, Li D H, Bao J, Deng D G, Guo H and Lei L 2022 *Chem. Commun.* **58** 2327
[15] Deng T T, Song E H, Zhou Y Y and Yuan J 2019 *J. Alloys Compd.* **795** 453
[16] Kim Y H, Arunkumar P, Kim B Y, Unithrattil S, Kim E, Moon S H, Hyun J Y, Kim K H, Lee D, Lee J S and Im W B 2017 *Nat. Mater.* **16** 543
[17] Ye W G, Ma C Y, Li Y B, Zhao C, Wang Y Z, Zuo C D, Wen Z C, Li Y K, Yuan X Y and Cao Y G 2021 *J. Mater. Chem. C* **9** 15201
[18] Zou H, Chen B, Hu Y F, Zhang Q W, Wang X S and Wang F 2020 *J. Phys. Chem. Lett.* **11** 3020
[19] Zou H, Yang X Q, Chen B, Du Y Y, Ren B Y, Sun X W, Qiao X S, Zhang Q W and Wang F 2019 *Angew. Chem. Int. Ed.* **58** 17255
[20] Zhou L J, Wang W X, Xu D K, Wang Z Y, Yi Z B, Wang M and Lu Z G 2021 *Ceram. Int.* **47** 34820
[21] Li X W, Xu H L, Xia X M, Xie F Y, Zhong S L and Xu D K 2019 *Ceram. Int.* **45** 10461
[22] Wang W, Fu M Q, Liu S W, Zhang X Y, Wei Y and Li G G 2022 *J. Lumin.* **242** 118536
[23] Evans J, Mary T A and Sleight A W 1998 *J. Solid State Chem.* **137** 148
[24] Shannon R D 1976 *Acta Crystallogr. A* **32** 751
[25] Tian Y, Chen B J, Hua R N, Sun J S, Cheng L H, Zhong H Y, Li X P, Zhang J S, Zheng Y F, Yu T T, Huang L B and Yu H Q 2011 *J. Appl. Phys.* **109** 053511
[26] Lal S C, Naseemabeevi J I and Ganesanpotti S 2021 *J. Am. Ceram. Soc.* **104** 5293
[27] Xie J H, Ding N, Li X B, Huang W T, Yang H J, Wang J, Wang L X and Zhang Q T 2019 *J. Mater. Sci-Mater. El.* **30** 17923
[28] Huang s H and Lou L R 1990 *Chin. J. Lumin.* **11** 1
[29] Tian Y, Chen B J, Tian B N, Hua R N, Sun J S, Cheng L H, Zhong H Y, Li X P, Zhang J S, Zheng Y F, Yu T T, Huang L B and Meng Q Y 2011 *J. Alloys Compd.* **509** 6096
[30] Mu B S, Zhang Y, Bian Q F, Li C R, Li Z C, Chu Y T, Zhao F and Sun J C 2021 *Chin. Phys. B* **30** 123201
[31] Wang C L, Jin Y H, Yuan L F, Wu H Y, Ju G F, Li Z Z, Liu D, Lv Y, Chen L and Hu Y H 2019 *Chem. Eng. J.* **374** 992
[32] Wang X F, Liu Q, Bu Y Y, Liu C S, Liu T and Yan X H 2015 *RSC Adv.* **5** 86219
[33] Rai V K 2007 *Appl. Phys. B-Lasers O.* **88** 297
[34] Vu Q T H, Bondzior B, Stefanska D, Miniajluk-Gawel N, Winiarski M J and Deren P J 2021 *Sci. Rep.* **11** 22847